Plant Physiology, April 2000, Vol. 122, pp. 1365–1377, www.plantphysiol.org © 2000 American Society of Plant Physiologists

Changes in Hechtian Strands in Cold-Hardened Cells Measured by Optical Microsurgery[1]

Charles S. Buer[2], Pamela J. Weathers*, and Grover A. Swartzlander, Jr.

Departments of Biology/Biotechnology (C.S.B., P.J.W.) and Physics (G.A.S.), Worcester Polytechnic Institute, 100 Institute Road, Worcester, Massachusetts 01609–2280

Optical microsurgical techniques were employed to investigate the mechanical properties of Hechtian strands in tobacco (*Nicotiana tabacum*) and *Ginkgo biloba* callus cells. Using optical tweezers, a 1.5-μm diameter microsphere coated with concanavalin A was inserted though an ablated hole in the cell wall of a plasmolyzed cell and attached to a Hechtian strand. By displacing the adhered microsphere from equilibrium using the optical trapping force, the tensions of individual strands were determined. Measurements were made using both normal and cold-hardened cells, and in both cases, tensions were on the order of 10^{-12} N. Significant differences were found in the binding strengths of cold-hardened and normal cultured cells. An increased number density of strands in cold-hardened *G. biloba* compared with normal cultured cells was also observed. Although no Hechtian strands were detected in any Arabidopsis callus cells, strands were present in leaf epidermal cells. Finally, the movement of attached microspheres was monitored along the outside of a strand while cycling the osmotic pressure.

Following plasmolysis of plant cells, it is often possible to detect thread-like strands connecting the cell wall to the plasmalemma, as first described by Pringsheim (1854) and Nägeli (1855). Hecht (1912), however, received credit for the discovery and the filaments were subsequently called Hechtian strands. Several authors have cited examples of Hechtian strands, since these early descriptions in various organisms, including algae, fungi, and higher plants (Bower, 1883; Burgess, 1971; Goosen-De Roo, 1973; Pont-Lezica et al., 1993; De Boer et al., 1994; Henry et al., 1996; Niu et al., 1996; Bachewich and Heath, 1997). To our knowledge, only three reports have described Hechtian strands in callus cells (Johnson-Flanagan and Singh, 1986; Chang et al., 1996; Buer, 1998).

Little is known about the function, composition, or physical properties of Hechtian strands. Their cross-sectional diameter ranges from 30 to 250 nm (Sitte, 1963; Oparka et al., 1994; Bachewich and Heath, 1997) and the length varies with the degree of plasmolysis and location within the individual cell. Oparka et al. (1994) suggested the strands conserve excess plasmalemma during plasmolysis. Using a fractal analysis with a time-dependent fractal dimension, they showed that Hechtian strands could account for the loss of surface area of the plasmalemma as plasmolysis occurs. On the other hand, Pont-Lezica et al. (1993) suggested two mechanical functions of the strands: maintenance of cell polarity by limiting slippage of the cytoplasm against the cell wall, and organization of deplasmolysis events providing an orderly restoration of cell function.

The strand's outer layer is plasmalemma, as seen by transmission electron microscopy using phosphotungstic acid (Sitte, 1963; Oparka et al., 1994; Bachewich and Heath, 1997). Some authors (Drake et al., 1978; Attree and Sheffield, 1985; Chang et al., 1996) have observed esterase activity within the strands using fluorescein diacetate (FDA), suggesting that they contain cytoplasm. Oparka et al. (1994), however, did not detect esterase activity in the strands of onion epidermal cells. 3,3′-Dihexyloxacarbocyanine iodide [$DiOC_6(3)$] fluorescence suggested that the interior of the strands is ER (Quader and Schnepf, 1986; Oparka et al., 1994). This fluorochrome is a known marker for mitochondria and ER in animal cells (Terasaki and Reese, 1992). Staehelin (1997) reviewed the functional domains of the ER and described a plasmalemma "anchoring domain." These sites have been shown to resist plasmolysis and remain coupled to the cell wall during the formation of Hechtian strands (Gunning and Steer, 1996; Oparka et al., 1996). Hepler et al. (1990) found no direct adhesion of the ER to the plasmalemma in lettuce using electron microscopy, although very close associations were present.

Schindler et al. (1989) hypothesized that wall-to-membrane linker proteins (integrin- and vitronectin-like) were binding sites of the plasmalemma to the cell wall. Canut et al. (1998) showed that RGD-containing peptides inhibited Hechtian strand formation in onion epidermal cells and altered the shape of the plasmalemma in plasmolyzed Arabidopsis callus cells. Others have suggested that motor proteins associated with the ER (actin filaments, Knebel et al., 1990, and Lichtscheidl et al., 1990; myosin, Liebe and Quader, 1994) may also provide adhesion points and subsequent Hechtian strand formation (Gunning and Steer, 1996).

Particularly interesting to our study were inferences that Hechtian strands undergo changes during cold hardening.

[1] This work was supported by the U.S. Department of Agriculture National Needs Fellowship (grant no. 93–38420–8804), the Research Corporation Cottrell Scholars Program, and the National Science Foundation (grant nos. BES 9414585 and ECS 9457481).

[2] Present address: Environmental Biology and Plant Cell Biology Groups, Research School of Biological Sciences, Building 46, The Australian National University, G.P.O. Box 475, Canberra ACT 2601, Australia.

* Corresponding author; e-mail weathers@wpi.edu; fax 508–831–5936.

Scarth (1941) and Johnson-Flanagan and Singh (1986) noted that the strands in unhardened cells broke more easily and were less numerous than in hardened cells. Their results suggested that strands become more elastic following cold acclimation.

A complete understanding of cold acclimation and freezing tolerance is lacking despite several decades of research. The induction of freezing tolerance and its loss during warming varies substantially between species, complicating this knowledge. Cold acclimation is necessary for cold-hardy plants to survive freezing temperatures. Several changes in physiological characteristics occur during the acclimation process (for recent reviews, see Alberdi and Corcuera, 1991; Hughes and Dunn, 1996; Li and Chen, 1998). For example, cold-responsive genes are activated (Thomashow, 1998), plasmalemma lipids show increased levels of unsaturation after growth at low temperatures (Tokuhisa et al., 1998), and the lipid composition and the ratio of lipid to protein in membranes change (Hughes and Dunn, 1996). Plants that can cold harden generally avoid membrane destabilization because changes in the lipids of the plasmalemma increase the cryostability of the cell (Uemura and Steponkus, 1998). A working hypothesis is that lipids in cold acclimated cells provide more elasticity to the plasmalemma, thereby allowing it to withstand rehydration during thaw cycles (Alberdi and Corcuera, 1991).

The time scale to achieve maximum hardiness varies between species. In spinach, a maximum freezing tolerance (approximately −18°C) was achieved after 1 to 3 weeks of low temperature exposure, whereas deacclimation was completed within 1 week (Guy, 1990). *Hedera helix* required 6 weeks to reach maximum cold tolerance and deacclimated in 1 week. Locust began achieving tolerance in August and reached maximum cold tolerance by mid-November in a natural setting in Japan, whereas a loss of tolerance took 2 months (Guy, 1990). The most rapid change has been shown to occur in as little as 1 d after low temperature exposure in Arabidopsis (Gilmore et al., 1988).

Using laser microsurgery and optical micromanipulation techniques, we have, for the first time to our knowledge, determined the elastic properties of Hechtian strands in hardened and unhardened cells. By adhering a microsphere to a strand and displacing the strand using "optical tweezers" (Ashkin et al., 1986), one may measure the tension and spring constant of a strand. Optical tweezers use laser light to produce non-contact forces in the piconewton range, and are capable of positioning small particles with submicrometer accuracy (for reviews, see Svoboda and Block, 1994; Hoffmann, 1996; Sheetz, 1998). Intracellular forces have previously been indirectly measured using organelles trapped in a focused laser beam (Ashkin and Dziedzic, 1989; Grabski et al., 1994; Schindler, 1995; Felgner et al., 1996), but the force was not calibrated.

Based on earlier reported lipid changes in cold-hardened cells, we expected to find differences between the elastic properties of the strands in our investigation: callus cells of a non-hardy species, tobacco (*Nicotiana tabacum*), and a cold-hardy species, *Ginkgo biloba*. Surprisingly, we found no significant difference in the spring constant, which was in the range of $k = 10^{-7}$ N m^{-1}, of either species after exposures to cold temperatures for prolonged periods of time. However, we did measure a marked increase in the binding strength between microspheres coated with concanavalin A (Con A) and strands following cold acclimation: 14% for *N. tabacum* and 31% for *G. biloba*. Similar to results from Scarth (1941) and Johnson-Flanagan and Singh (1986), we detected an increased number density of strands in cold-hardened *G. biloba* compared with the other species we studied. In addition to our measurements of tension and binding strength, we developed a means to observe physiological dynamics of a strand during deplasmolysis/replasmolysis cycles by monitoring multiple microspheres attached to individual Hechtian strands.

MATERIALS AND METHODS

Plant Cell Culture

Ginkgo biloba callus, initiated from a seedling hypocotyl, was grown according to the method of Carrier et al. (1990) and Johnson (1994) in liquid Murashige and Skoog Minimum Organics (MSMO) basal salts (Linsmaier and Skoog, 1965) supplemented with Suc (3%, w/v) and agitated at 100 rpm on a rotary shaker. Kinetin (1 mg L^{-1}) and naphthylacetic acid (NAA) (2 mg L^{-1}) were added as plant growth regulators, and the pH was adjusted to 6.0 with 2 M NaOH before autoclaving.

Tobacco (*Nicotiana tabacum*) callus was maintained on semi-solid (Gelrite, Adams Scientific, West Warwick, RI, or Phytagel, Sigma Chemical, St. Louis; 0.4%, w/v) Murashige and Skoog (MS) basal salts medium (Murashige and Skoog, 1962), supplemented with Suc (3%, w/v) and casein hydrolysate (1 g L^{-1}). Kinetin (0.2 mg L^{-1}) and indole-3-acetic acid (IAA) (2 mg L^{-1}) were added as growth regulators. The pH was adjusted to 5.8 before autoclaving.

Arabidopsis ecotype Columbia callus was initiated from seedlings and maintained in culture according to the methods of Akama et al. (1992). Hechtian strands were observed in cells of epidermal peels of the oldest leaves from 10-d-old seedlings.

All plant tissues were grown under continuous cool-white fluorescent lights (20 μmol m^{-2} s^{-1}) at 25°C. Hechtian strands were found most readily in actively growing cells, so all tissues were subcultured at 2- to 4-week intervals. Cold-hardened cells were grown at 25°C for 1 week following subculture and then transferred to and maintained at 5°C ± 2°C at similar light levels for a minimum of 1 week before experimentation.

Visual observations of cytoplasmic streaming and plasmolysis/deplasmolysis were used to determine cell viability. Only living cells are capable of cytoplasmic streaming and can deplasmolyze from a plasmolyzed state (Lee-Stadelmann and Stadelmann, 1989; Kuroda, 1990).

Callus cell plasmolysis was accomplished using a step gradient varied from 0.1 → 0.2 → 0.3 → 0.4 M NaCl with a minimum of 5-min (usually 10 min) intervals between steps. All concentrations of the step gradient also contained 10 mM Tris (pH 7.2), 10 mM $CaCl_2$, and 10 mM $MnCl_2$. Plasmolysis/deplasmolysis cycle experiments were performed using a smaller step: 0.4 → 0.35 → 0.3 M NaCl.

Microsphere Insertion

The optical system (Fig. 1), included a pulsed (30 Hz), seeded Nd:YAG laser (model GCR 170, Spectra-Physics, Mountain View, CA) with second and third harmonic generation capabilities (for details, see Buer et al., 1998). The stationary fundamental Gaussian beam (1064 nm, long pulse mode, 200-μs duration) was used for trapping polystyrene microspheres, and the frequency tripled beam (355 nm, Q-switched, 6-ns duration pulse) was used to ablate a hole through the cell wall. The laser beams were collimated with uncoated lenses (BK-7 glass), directed through a series of beam steering prisms (BK-7 glass), and focused with a $\times$100 (numerical aperture 1.3) oil immersion microscope objective (Neofluar, Carl Zeiss, Thornwood, NY) to a nearly diffraction-limited spot (about 1 wavelength in diameter). The objective was also used to image the working area onto a CCD camera, and provided a depth of field of approximately 1 μm. A beam stop was used to prevent the simultaneous illumination of the sample at both wavelengths. Optical trapping and ablation operations were performed following the method of Buer et al. (1998) using a flow chamber (Walcerz and Diller, 1991) to immobilize the cells and allow variable osmotic concentrations.

Preparation of Con A-Coated Microspheres

Microspheres were surfactant-free, carboxylated white polystyrene latex of diameter (D) = 1.50 $\pm$ 0.08 μm (P/N 7–1600, Interfacial Dynamics, Portland, OR). Even though the particles are charged, the hydrophobic latex binds strongly to hydrophobic molecules. The negative surface charge is pH dependent (stable at neutral to high pH). The microspheres were coated with Con A (type V, product no. C7275, Sigma) following the protocol of Kucik et al. (1991). Microspheres (100-μL suspension) were transferred into 1 mL of Con A (2 mg mL^{-1} in 200 mM Tris, pH 7.2), shaken on ice for 3 h, centrifuged (10,000g, 3 min), resuspended in bovine serum albumin (BSA) (5 mg mL^{-1} in 200 mM Tris, pH 7.2), and washed twice by centrifugation. The microspheres were resuspended in a 10-mL solution of 0.4 M NaCl, 10 mM Tris, pH 7.2, 10 mM $CaCl_2$, 10 mM $MnCl_2$ (Ca^{2+} and Mn^{2+} are essential cofactors for Con A activity; Goldstein and Poretz, 1986), and calcofluor (0.01%, w/v, De Boer et al., 1994), resulting in a final concentration of approximately 2 $\times$ 10^{10} microspheres mL^{-1}. The microspheres and Con A solution were stored at 4°C. Freshly coated microspheres were prepared for each day's experiments. Unused Con A was stored desiccated below 0°C. Negative controls (uncoated and BSA-coated microspheres) verified that Con A was the binding factor to Hechtian strands.

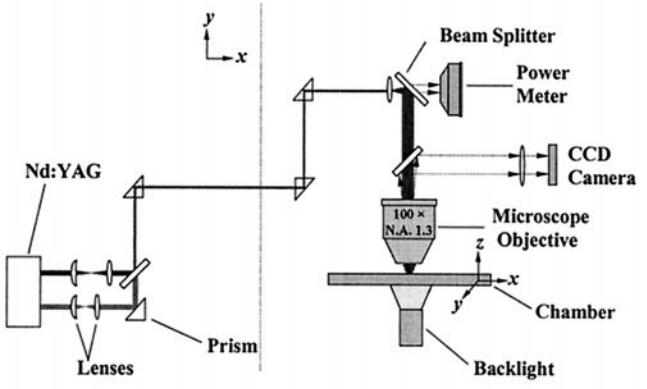

Figure 1. Schematic of the optical system. A Nd:YAG laser supplies a Q-switched UV beam for ablating a hole through the cell wall and a long-pulsed infrared beam for optical trapping of polystyrene microspheres. The beam is directed to a $\times$100 microscope objective, and the beam forms a focal spot within a chamber containing callus cells. Backlighting the chamber allows the objective to image the trapping region onto a CCD camera.

Calibration of Trapping Force

The effective trapping force exerted on a microsphere may be determined by calibrating the system against a viscous drag force (Wright et al., 1994). We used a computer-controlled actuator (StepperMike, model 18510, Oriel, Stratford, CT) to accelerate ($a \approx 1$ μm s^{-2}) the entire trapping chamber (including the fluid within it) so that a trapped stationary particle would experience viscous drag from the moving fluid. To minimize vibrations, a compact translation stage assembly was used. Microscope chambers (CoverWell PCI-0.5, Grace Bio-Labs, Sunrise, OR) were used instead of the massive flow chamber. A no. 1½ coverslip (25 $\times$ 25 mm) was used to seal the top of the microscope chamber and allow light transmission. The critical velocity at which viscous drag overcomes the trapping force (v_{cr}) was obtained from the actuator controller display. The maximum effective trapping force ($F_{trap} = F_{drag}$) was calculated from Stokes' Law: $F_{drag} = 6\pi\mu R_p v_{cr}$, where μ is the viscosity of the surrounding aqueous solution (approximately 1.20 $\times$ 10^{-3} Ns m^{-2} for 0.4 M NaCl, 20°C; Munson et al., 1994), and $R_p = \frac{1}{2}D = 0.75 \pm 0.04$ μm is the radius of the microsphere. This experiment was repeated at least 20 times at a given laser beam energy (E_{beam}) to obtain an average relation with F_{trap}, resulting in a precision of $\pm$15% (Fig. 2). The value of E_{beam} was varied from the trapping threshold of 50 μJ to 350 μJ (or until damage occurred). The calibration differs with trapping depth due to optical aberrations. To account for the decreased trapping strength with increasing depth, we made measurements at depths of 20, 40, 60, and 80 μm below the coverslip. At depths $<$20 μm boundary effects perturb the calibration (Mehta et al., 1998), and at depths exceeding 80 μm we were unable to effectively trap a microsphere with the available energy of our laser. The microspheres were optically damaged at energies exceeding 250 μJ when the trapping depth was less than 40 μm.

The microscope objective in our apparatus (Fig. 1) serves two purposes: to form the optical trap and to image microscopic features onto a video camera. The video images of a microsphere attached to a Hechtian strand (Fig. 3), therefore, shows the perspective in the reference frame of the trapped microsphere. The values of displacement and strand length, Δx and L, respectively, were determined after calibrating image distances with 10-μm cross-hairs on

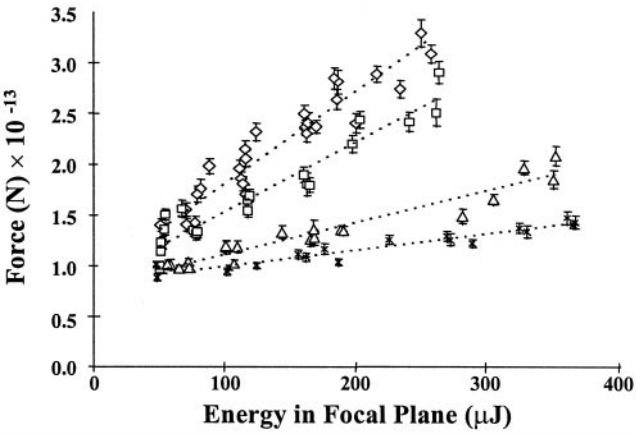

Figure 2. Calibration of average trapping force versus energy in the focal plane for 1.5-μm diameter Con A-coated polystyrene microspheres using Stokes' Law following the method of Wright et al. (1994). Error bars are the SE of the mean of at least 20 separate trials in 0.4 M NaCl, 10 mM Tris, pH 7.2, 0.01% (w/v) calcofluor, 10 mM $CaCl_2$, and 10 mM $MnCl_2$. ◇, 20 μm depth; □, 40 μm depth; △, 60 μm depth; ×, 80 μm depth.

the microscope objective. For example, a distance of 1 mm on the television monitor corresponded to 0.2 μm at high magnification. A precision of approximately $\pm$0.1 μm was achieved for transverse distances. A video cassette recorder (model SLV 660HF, Sony, Park Ridge, NJ) was used to store the images on videotape at the standard rate of 30 frames s^{-1}, and video play-back allowed us to perform frame-by-frame analyses. Measurements were made at chamber temperatures of approximately 20°C and approximately 10°C for normal and hardened cells. To prevent water condensation on the trapping chamber, the coverslip was wiped with immersion oil, and the room temperature was lowered to approximately 15°C. All trapping measurements were repeated at least five times to obtain reliable average values.

Number Density Determination

The selected cells used in all parts of this study were: (a) cells that were adequately isolated from the callus mass (to provide sufficient back-lighting, allow unobstructed ablation, and facilitate insertion of microspheres), (b) cells that could be plasmolyzed to approximately 70% of the original volume (at 0.4 M NaCl), and (c) cells that remained $\geq$1 h in the plasmolyzed state (assumed to have reached a stable condition).

The mean number density was determined by counting the number of observed strands in an optical section under high magnification, and dividing by the arc length of the observed region of the cell wall and the apparent depth of field (estimated to be 1 μm). We averaged over strands of any length and over repeated measurements at different focal depths. Unresolved strands probably did not exist, otherwise we would have encountered invisible structures blocking the motion of the optically trapped microspheres as they were moved throughout the plasmolysis-induced void space (PVS).

Assays of Strands for Cytoplasm, ER, and F-Actin

Prior to all assays, callus cells of *N. tabacum* and *G. biloba* were plasmolyzed to 0.4 M NaCl using the normal step gradient described above to yield well-defined Hechtian strands. FDA (Fluka Biochemika, Buchs, Switzerland) at the same concentrations used for cell viability (Widholm, 1972) was used to test for cytoplasm in Hechtian strands. Cells were illuminated with the 488-nm line of an Ar^{+} laser. Blue light was blocked at the CCD camera (Fig. 1) with a 3-69 glass filter (Corning Glass, Corning, NY) to allow the detection of fluorescence from the cells.

$DiOC_6(3)$ (1 μg mL^{-1}, Sigma) was used to determine the presence of ER in Hechtian strands according to the method of Quader and Schnepf (1986). Cells were illumi-

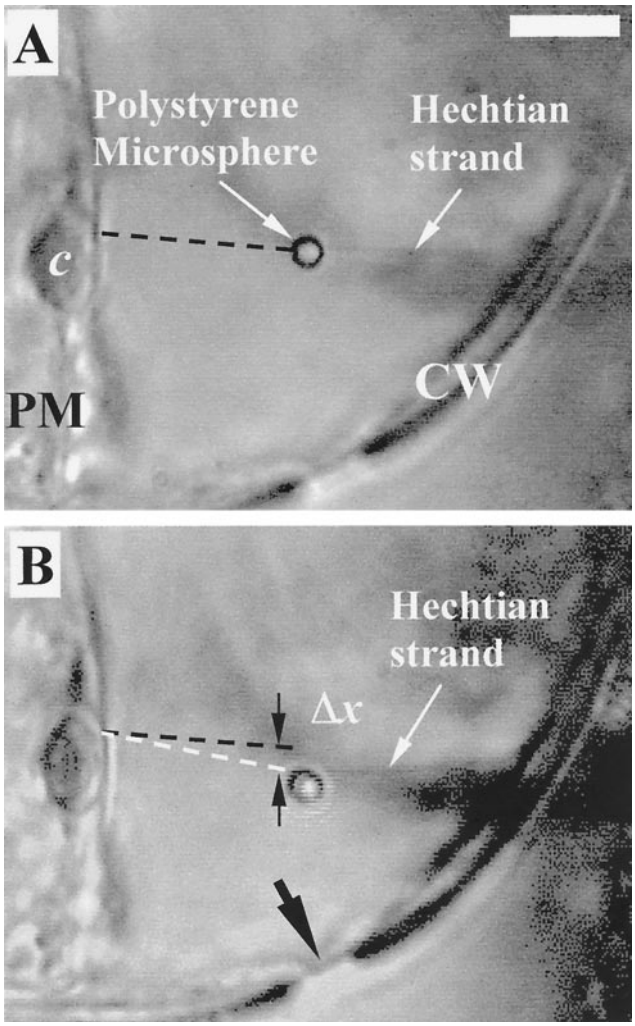

Figure 3. Videotape frames showing a Hechtian strand (with an attached 1.5-μm diameter polystyrene microsphere) between the cell wall (CW) and plasmalemma (PM) of a plasmolyzed *Ginkgo biloba* cell. A, Equilibrium position (no displacement) showing the relative position of the strand (dashed black line) with a convenient chloroplast (*c*). Strand displaced by a distance, Δx (B, dashed white line) compared with the equilibrium position (A). The ablated hole though which the microsphere was manipulated is marked in B (arrow). Bar is 5 μm.

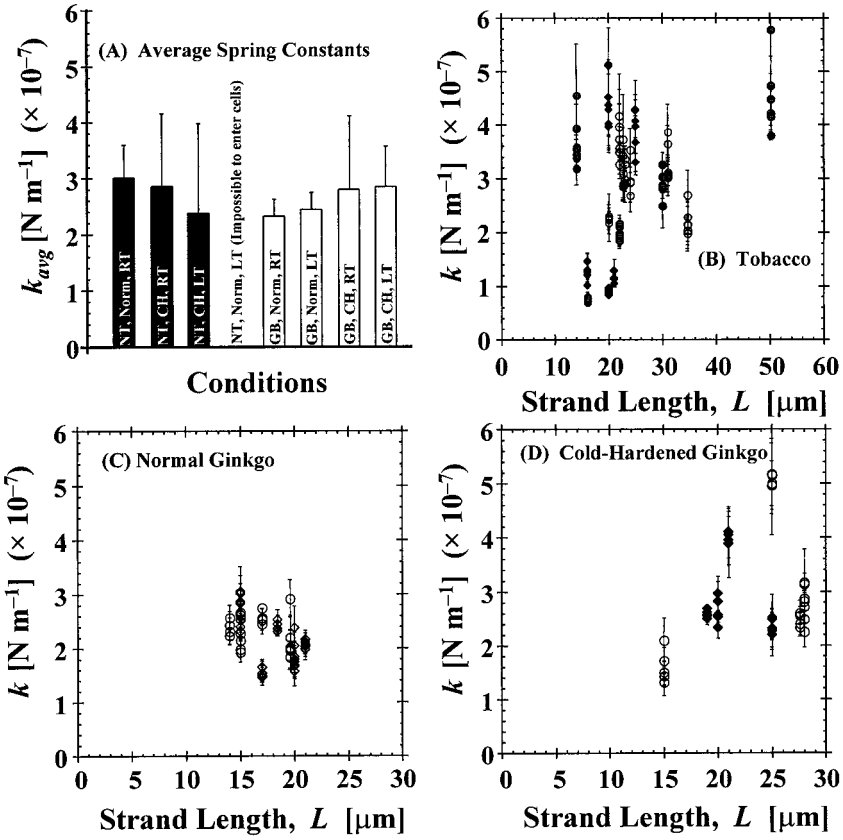

Figure 4. Measured values of the spring constant (k) when a Hechtian strand of length L is transversely displaced from equilibrium. Measurements were made at room temperature (RT) at approximately 20°C (circles) and low temperature (LT) at approximately 10°C (diamonds). Values of k for normal (Norm) RT, ○; cold-hardened (CH), LT, ●, and Norm LT, ◆, for tobacco, (B); Norm *G. biloba* (GB) RT, ○, and Norm GB LT, ◇, (C); and cold-hardened *G. biloba*, RT, ○, and LT, ◆ (D).

nated with 488 nm of light from the Ar^+ laser and viewed at ×2,000 magnification. Cells were assayed ≥0.5 h following the introduction of $DiOC_6(3)$.

N-7-nitrobenz-2-oxa-1,3-diazol-4-yl phallacidin (NBD-ph) (Molecular Probes, Eugene, OR) was used to test for the presence of F-actin in Hechtian strands following the protocol of Barak et al. (1980) for living cells; 10 mg mL^{-1} *p*-phenylenediamine was added to reduce photobleaching (Heath, 1987). After incubation (≥1 h), fluorescence was initiated with the 488-nm line and blue light was blocked as previously described.

RESULTS AND DISCUSSION

Tension in the Hechtian Strands

To determine the elastic properties of a Hechtian strand, we performed a classic measurement similar to plucking a string (Fig. 3). A microsphere was attached at the center of the strand and slowly translated perpendicular to the strand axis. At the position where the tension in the strand equals the trapping force, the microsphere is pulled out of the optical trap. We assume the strand obeys Hooke's Law, $F = -k\,\Delta x$, where F is the restoring force of the strand and is equal in magnitude to the maximum transverse trapping force when $\Delta x = \Delta x_{max}$, and where Δx_{max} is the displacement from the equilibrium position when the microsphere is pulled out of the trap, i.e. $F_{trap} = k\,\Delta x_{max}$. Once released from the trap, the strand retracts to its equilibrium position without oscillating. This maximum displacement was measured over a range of laser energies to determine the average value of the spring constant (k) for a given strand of length, L (measured from a center point on the cell wall to a center point on the plasmalemma). Experimentally, we find $\Delta x_{max} \ll L$, and thus Hooke's Law is expected to be valid. Since the strand is in equilibrium, the tension (T) must balance the applied force and, thus, we find $T = \frac{1}{4}kL$.

For simple elastic bodies, k may be expressed in terms of the elastic modulus (E) $k = 12A^2E/\pi L^3$, where A is the cross-sectional area of the strand (Landau and Lifshitz, 1959; Kelly, 1993). The longer the strand of a given elasticity, the easier it is displaced from equilibrium. Hechtian strands, however, are not simple bodies. For example, the strand may lengthen by adding more mass or by stretching as the cell plasmolyzes.

We assume the main source of strand tension is the differential pressure across the plasmalemma (ΔP) resulting from the cell's effort to make osmotic adjustments. Although we recognize that plant cells have irregular shapes and do not exhibit uniform plasmolysis, the essential physics may be understood by developing a model based on a spherical callus cell. The tension may be expressed as $T = \eta^{-1}\,\Delta P\,(1 - L/R_0)^2$, where R_0 is the radius of the cell and η is the number of strands per unit area along the cell wall. As the value of L approaches R_0, one may expect that strands will break, and thus the tension in each remaining strand will increase to balance the pres-

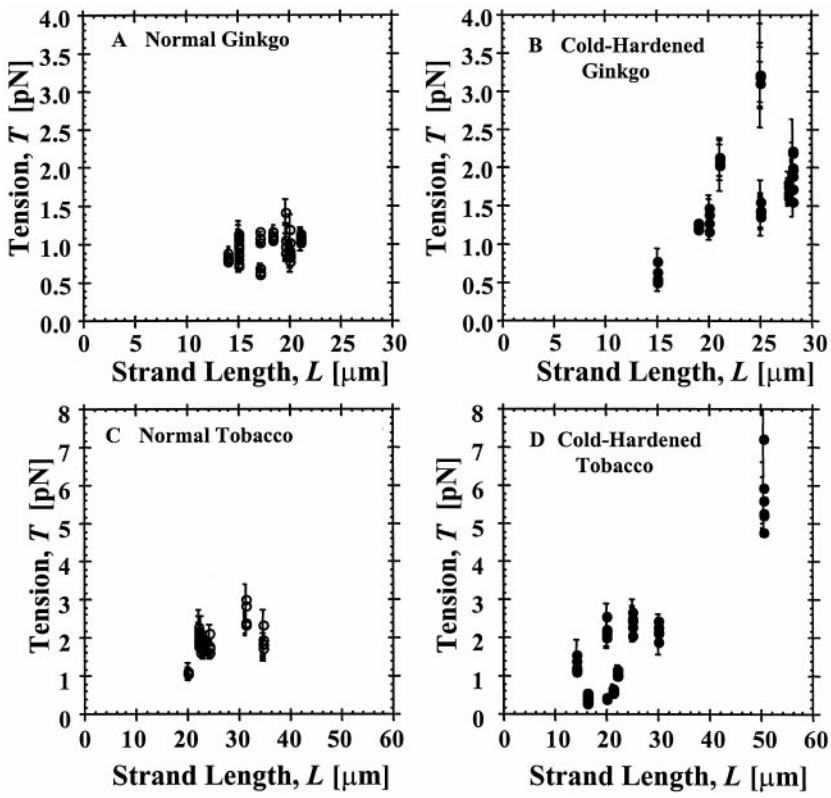

Figure 5. Measured values of the tension in Hechtian strands for normal *G. biloba* (A), cold-hardened *G. biloba* (B), normal *N. tabacum* (C), and cold-hardened *N. tabacum* (D).

sure. This will also occur if the strands merge together. Assuming a simple linear decrease in the strand population, $\eta = \eta_0(1 - L/L_{cr})$, where η_0 is the initial strand density and L_{cr} is a material-dependent parameter that characterizes the critical distance at which no strands remain (due to breakage or coalescing), we find that the tension,

$$T = (1/4)kL = \Delta P(1 - L/R_0)^2/\eta_0(1 - L/L_{cr})$$

may either increase or decrease with L, depending on the value of L_{cr}. When $L_{cr} < R_0$ the tension increases to infinity at $L = L_{cr}$, and the tension increases monotonically (i.e. $dT/dL > 0$) if $L_{cr} < \frac{1}{2}R_0$; otherwise, the tension initially decreases for small values of L, and then increases monotonically. Thus, one may expect the observed tension to: (a) increase rapidly with strand length in cells containing easily broken or merged strands; (b) remain relatively constant in cells with moderate resistance to coalescing and breakage; and (c) slowly decrease for short strand lengths and rapidly increase for long strand lengths in cells having strong strands that do not merge.

Experimentally, the tension is determined by evaluating the expression, $T = \frac{1}{4}kL$, where $k = F_{trap}/\Delta x_{max}$, F_{trap} is known from the beam energy and the calibration curves (Fig. 2), and Δx_{max} and L are measured from the microscope images. At the upper range of values of the applied trapping force, the microsphere would sometimes detach from the strand. Furthermore, attached microspheres easily detach if displaced parallel to the strand, and thus direct measurements of the Young's modulus were not possible using optical tweezers.

The determined values of k and T are shown in Figures 4 and 5, respectively, for normal and cold-hardened cells. Surprisingly, the average values of the spring constants for *G. biloba* and *N. tabacum*, shown in Figure 4A, were statistically indistinguishable, and the spring constants did not change significantly after cold hardening. Measurements taken at low (10°C) and room (20°C) temperature were also indistinguishable. Even within the same cell, significant differences in tension were found for different strands (data not shown). We attribute this variation to: (a) naturally occurring differences between strands (such as the strand length and diameter), and (b) relaxation of the tension over time due to natural deplasmolysis. Averaging the mean spring constants gave a value $k_{avg} = 2.7 \times 10^{-7}$ N m^{-1} and a SD of ±10%.

In all cases, the tension (Fig. 5) was $T \approx 1 - 2$ pN when $L = 20$ μm. These plots suggest that in cold-hardened cells, the tension increases with strand length. This trend was not evident in normal cultured cells because either the effect is weaker or the range of strand lengths was too small. In *G. biloba*, the ranges of length for the normal and cold-hardened data overlap and, thus, based on our discussion above, we conclude that strands in normal cells are less prone to breaking or coalescing than those in hardened cells. The population of strands in a given cell (or equivalently the population density, η) decreases more readily in cold-hardened cells. Indeed, this was qualitatively verified by our observation that strands sometimes appeared

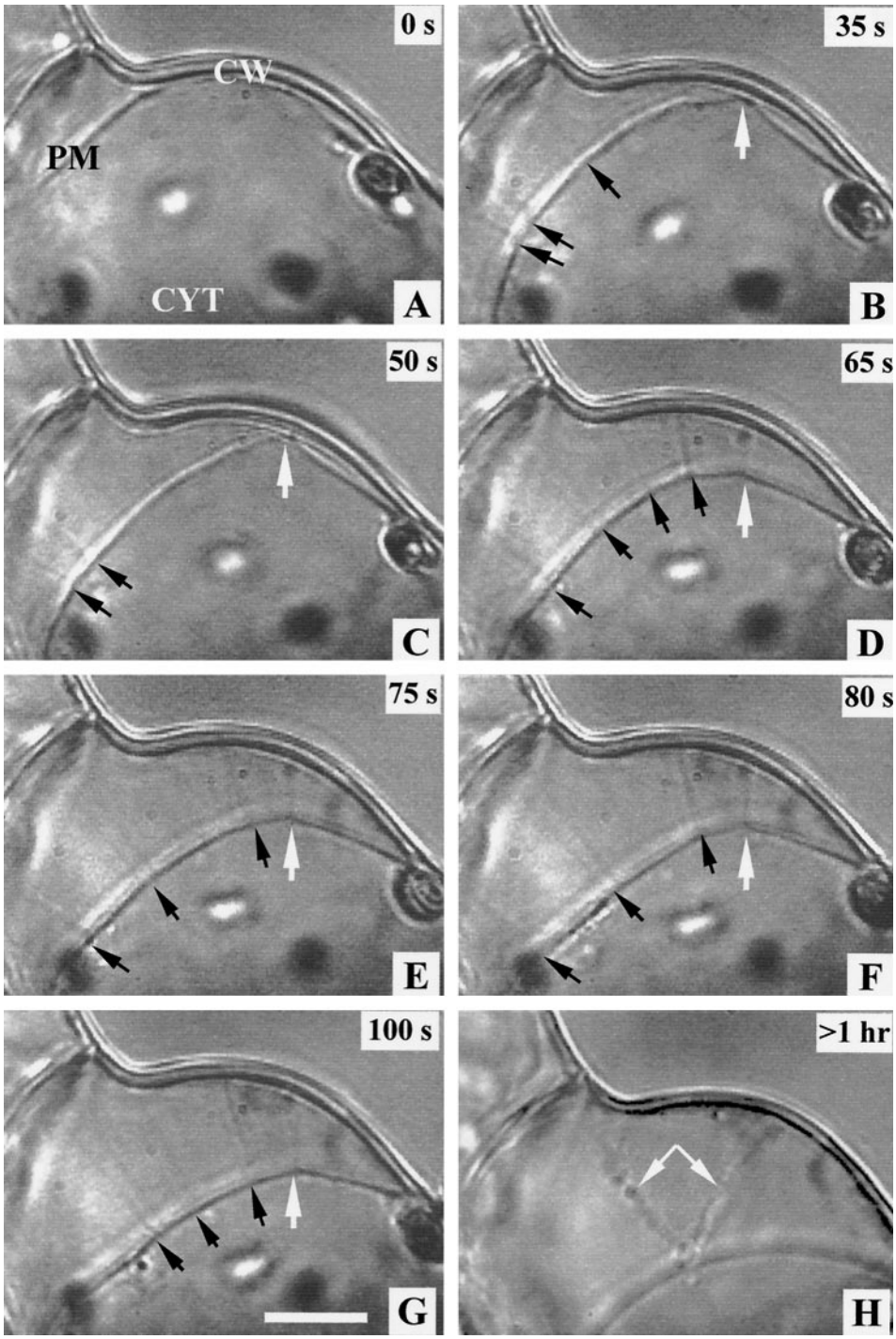

Figure 6. Sequence from videotape of a normal cultured *N. tabacum* callus cell showing Hechtian strand formation during plasmolysis. A, Incipient plasmolysis at 0.3 M NaCl. B through G, Plasmolysis with the gradual introduction of 0.4 M NaCl. Time of sequence is indicated in the upper right corners, and strands are at small arrows. Photograph of the same cell about an hour later showing changes in the strands (H, arrows). An apparent strong attachment point (B–G, large arrow) has disappeared in H. These strands were not used for tension measurements. The apparent depth of field is approximately 1 μm. CYT, Cytoplasm; PM, plasma membrane; and CW, cell wall. Bar is 10 μm.

thicker (maybe due to finer strands joining together to yield thicker strands, Fig. 6) when the cells were cold-hardened or when the strand length was very long.

Since rapid changes can occur in cells during cold acclimation (Gilmore et al., 1988; Guy, 1990; Zabotin et al., 1998), we also measured transitory effects by testing *G. biloba* and *N. tabacum* strand tensions at room temperature and cold temperatures for normal cultured and cold-

Table I. *Comparisons of the relative population, number density, and binding force for Hechtian strands in normal and cold-hardened cells*

The total number of observed cells is shown in parentheses. Different superscript letters indicate that a significant difference exists between individual conditions within columns. The strand frequency ($P < 2.2 \times 10^{-7}$) and maximum binding force ($P < 0.01$) in cold *G. biloba* were significantly higher compared with the other categories. The statistical comparisons were by the Student's *t* test.

Cell Type	Relative Population of Cells with Strands[a]	Mean No. Density	Average Maximum Binding Force ($n \geq 8$)
	average %	*no. μm^{-2} cell wall*	*(N) × 10^{-13}*
N. tabacum			
Normal callus	49.2 ± 19.8 ($n = 103$)[a]	0.065 ± 0.001 ($n = 21$)[a]	2.74 ± 0.46[a]
Hardened callus	44.2 ± 18.9 ($n = 119$)[a]	0.066 ± 0.001 ($n = 27$)[a]	3.20 ± 0.15[b]
G. biloba			
Normal callus	50.7 ± 24.2 ($n = 173$)[a]	0.061 ± 0.001 ($n = 19$)[a]	2.20 ± 0.14[a]
Hardened callus	24.3 ± 9.8[b] ($n = 142$)[b]	0.150 ± 0.002 ($n = 15$)[b]	3.19 ± 0.12[b]
Arabidopsis			
Normal callus	0 ($n = 146$)[c]		
Hardened callus	0 ($n = 88$)[c]		
Leaf epidermal cells[c]	39 ($n = 41$)[d]	Not tested	Not tested

[a] Sampled cells are only those optimally located in the callus mass. [b] The strands are very thin and numerous. [c] 10 d post germination. [d] Tested for presence only.

hardened cells. We were unable to insert microspheres into the PVS and perform measurements on normal cultured *N. tabacum* at cold temperatures. This was attributed to an unexpected phenomenon: a strong flow of liquid from the ablated hole that persisted for hours. Normally, after ablating a hole roughly the size of the microsphere, this flow subsided after a few minutes. We were still unable to introduce microspheres after doubling the width of the hole. Apparently, the decreasing temperature triggers a mechanism that boosts the pressure within the cell. Perhaps this activity is related to our inability to maintain *N. tabacum* callus cultures for more than 2 weeks at 5°C.

Strand Population Dynamics and Number Density

Hechtian strands were investigated in *G. biloba*, *N. tabacum*, and Arabidopsis grown under normal and cold-hardening conditions. Roughly 50% of the normal callus cells of *G. biloba* and *N. tabacum* had detectable Hechtian strands (Table I). Statistical analysis was performed using the Student's *t* test by comparing the means of data collected and assuming a normal distribution. Neither the normal nor cold-hardened Arabidopsis callus cells produced observable strands at magnifications up to ×4,000 (although they were observed in leaf epidermal cells). Remarkably, the population of cells producing strands in cold-hardened *G. biloba* dropped in half to roughly 25% ($P < 0.006$), whereas the decrease in *N. tabacum* was not significant. Compared with normal callus, we also found a 2.5-fold increase in the mean number density of strands in cold-hardened *G. biloba* (Table I), thus confirming the work of others (Scarth, 1941; Johnson-Flanagan and Singh, 1986). According to our discussion of strand tension above, one may expect less tension in cold-hardened *G. biloba* for short strand lengths due to the increased number of strands. Indeed, a comparison of Figure 5, A and B, supports this expectation at $L \approx 15$ μm.

Hechtian strands became visible with the onset of plasmolysis (Fig. 6), in contrast to some previous reports. Bower (1883) mentioned several plant species in which no strands were visible until 30 min or more had passed after plasmolysis. He hypothesized that individual strands coalesced to form thicker strands, thereby making them visible. During plasmolysis we did not observe the formation of additional strands, nor did we observe strands merging to produce thicker strands. However, thick, slow-moving plasmalemma sheets persisting across the PVS after plasmolysis in cold-hardened cells were seen to merge; the mass of these particular structures precluded their use in our measurements. After a prolonged state of plasmolysis (>1 h), we discovered that some strands disappeared (Fig. 6), as reported by others (Bower, 1883; Plowe, 1931; De Boer et al., 1994). We suspect fine Hechtian strands may merge, perhaps accounting for the apparent disappearance of thin strands and the appearance of thick strands during prolonged plasmolysis (Fig. 6). Strand breakage and absorption could also account for strand disappearance. However, strands present after more than 1 h were observed to remain intact for as long as 12 h in the plasmolyzed state, suggesting that the strands had reached a stabilized state. Only stabilized strands were used in our experiments.

Earlier, Johnson-Flanagan and Singh (1986) reported using 0.2 M increments of $NaCl:CaCl_2$ (9:1) to minimize strand breakage in *Brassica napus*. We also found that the use of a gradual step gradient minimized strand breakage, allowing strands to remain intact in >95% of strand-producing cells. Consequently, we used slow plasmolysis to provide the most consistent strands for our experiments. In contrast, rapid plasmolysis (directly increasing from 0.1-0.4 M NaCl or a rapidly applied step gradient) caused the strands to break or fail to be observed in most tested cells.

These results suggest that the number of Hechtian strands in a given cell is determined before the onset of plasmolysis. This number may decrease due to breakage or coalescence; however, to our knowledge, the formation of additional strands has only been observed after plasmoly-

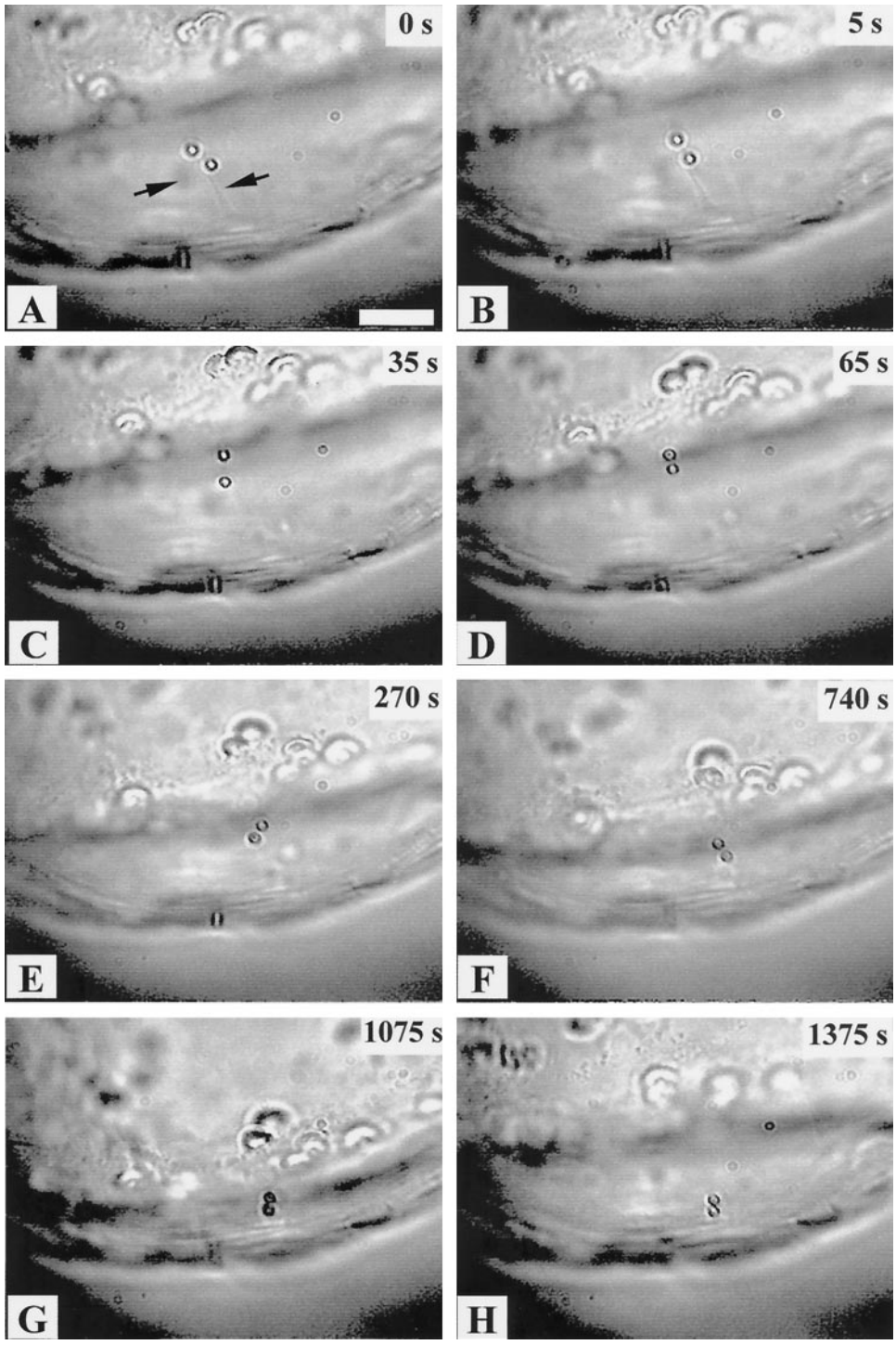

Figure 7. Sequence from a videotape of a typical deplasmolysis/replasmolysis experiment with 1.5 μm-diameter Con A-coated microspheres attached to the same Hechtian strand (A, arrows). A plot of the microsphere movement for this sequence is shown in Figure 8. Time of the sequence is in the upper right-hand corner of each frame. A through C, 0.4 → 0.35 M NaCl step-gradient; D and E, 0.35 → 0.3 M NaCl; F, 0.3 M, just before introduction of 0.35 M NaCl; G and H, 0.35 → 0.4 M NaCl gradient. Bar is 10 μm.

sis (Plowe, 1931) and then only by re-contacting the protoplast to the cell wall with microdissection needles. Thus, the hypothesis that Hechtian strands conserve excess plasmalemma during plasmolysis (Oparka, 1994) is not supported by this finding. Kell and Glaser (1993) describe an alternative mechanism for plasmalemma conservation, endocytotic vesiculation that has been shown to occur in isolated protoplasts. Upon deplasmolysis, incorporation of

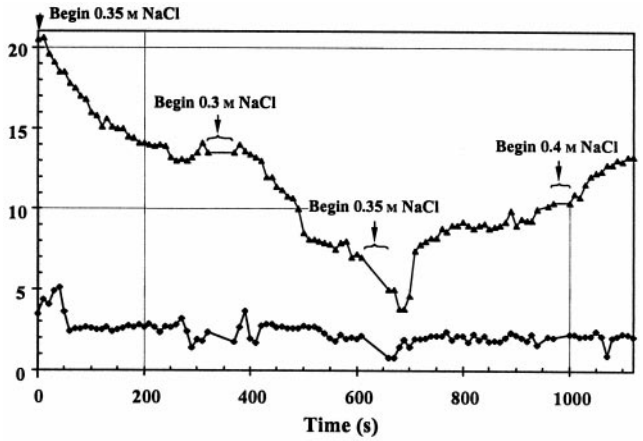

Figure 8. Measured distances between the centers of the attached microspheres (♦) and the position of the protoplast (with respect to the cell wall) as the cell first deplasmolyzes (0–610 s) and then replasmolyzes (660–1,120 s), corresponding to Figure 7 (▲). Varying the concentration of NaCl in steps controlled the osmotic pressure. Distance measurements have an uncertainty of ±0.5 μm. The mean distance between the microspheres is 2.7 ± 0.7 μm and 2.0 ± 0.4 μm during deplasmolysis and replasmolysis, respectively.

excess plasmalemma into the expanding membrane is necessary to prevent lysis. Lysis was never observed in our work.

Microsphere to Strand Binding Strength

Carboxylated polystyrene microspheres bind the plant lectin Con A through hydrophobic interactions at neutral or higher pH (Interfacial Dynamics catalog, 1997–1998). Furthermore, Con A selectively binds sugars with the following order of affinity: Man α-1,2-Man α-1,2-Man > Man α-1,2-Man > α-Man > α-Gluc > GlcNAc (Goldstein and Poretz, 1986). Therefore, Con A should bind to glycoproteins associated with the plasmalemma. Indeed, such binding was observed, whereas negative controls (uncoated and BSA-coated microspheres) did not adhere to the Hechtian strands or to the plasmalemma.

To attach optically trapped microspheres to a Hechtian strand, we positioned the microsphere above the strand and lowered the focal plane of the beam. Once attached, the microsphere became defocused when the trapping point was displaced from the strand. A period of approximately 20 s was often required to secure the microsphere, although on some occasions, binding occurred immediately.

The binding force between the microsphere and the strand was determined by increasing the optical trapping force until it had sufficient strength to detach the sphere. This measurement was made while pulling the microsphere perpendicular to the length of the strand. We noticed that the microsphere could be more easily detached by translating it along the length of the strand. However, the physical effects of a shear force on the connection between the microsphere and the strand are unknown. On the average, we found that cold-hardened cells had higher binding strengths than normal cells (Table I). This difference was particularly evident for *G. biloba*, in which the binding forces increased by a factor of 1.45 ± 0.11; for *N. tabacum* the enhancement factor was less than the relative error. This increase suggests a greater density of glycobearing binding substances on the strands, as reported by Castonguay et al. (1998). In some cases the sphere would not detach from the strand when the largest optical trapping force was applied. We never observed a strand breaking when perturbed with the optical tweezers, nor did we observe a displacement of the cell wall or protoplast from forced displacements of the strand.

Deplasmolysis Experiments

To explore possible relationships between the plasmalemma and Hechtian strands, we monitored the motion of microspheres attached to the strands during deplasmolysis/replasmolysis cycles. A video sequence of such a plasmolysis cycle is shown in Figure 7 with two microspheres attached to the same strand. The distance (along the strand) between the protoplast and the stationary cell wall, as well as the distance between the centers of the microspheres, is plotted as a function of time in Figure 8. In the latter case, a separation less than the sphere diameter indicates that one sphere moves behind the other. Within the first minute of deplasmolysis, the sphere distance initially increases from 3.5 to 5.0 μm, and then decreases to an average value of 2.7 ± 0.7 μm over the 10-min deplasmolysis period. During replasmolysis, little relative motion of the spheres was observed, and their separation was roughly constant, averaging 2.0 ± 0.4 μm.

Individual glycoproteins are thought to move independently on the fluid mosaic lipid bilayer of the plasmalemma (Singer and Nicolson, 1972). This is supported by our observations in Figures 7 and 8, which indicate that the microspheres can move independently.

Based on a series of such experiments (Table II), we observed that the microspheres migrated and adhered to the protoplast 43% of the time and to the cell wall 57% of the time. In about half of the experiments (n = 18) the strands broke before deplasmolysis was completed. After the strand broke, the microspheres were just as likely to move to the cell wall as toward the protoplast. In about 10% of the cells having attached microspheres, deplasmolysis did not occur due to cell death.

Table II. *Microsphere movements while attached to Hechtian strands during deplasmolysis/replasmolysis cycling experiments (n = 32)*

Result	Frequency
	%
Hechtian strands remained intact during cycling (n = 11)	34
Microspheres migrated to protoplast (n = 5)	45
Microspheres migrated to cell wall (n = 6)	55
Hechtian strands broke during deplasmolysis[a] (n = 18)	56
Microspheres moved toward protoplast (n = 9)	50
Microspheres moved toward cell wall (n = 9)	50
No replasmolysis/deplasmolysis (perished) (n = 3)	10

[a] Microsphere velocity >13 μm s^{-1} immediately after breakage.

These results suggest that the strand contents may be absorbed by the protoplast during deplasmolysis. In cases when deplasmolysis rates are sufficiently slow, tension remains in the strand as it is apparently absorbed and, thus, the protoplast eventually meets the microsphere. When the deplasmolysis rate is too fast, the strand loses tension and the microsphere may drift toward either the protoplast or the cell wall.

Interestingly, on one occasion we filmed the breakage of a strand having two attached microspheres as the cell replasmolyzed. Using the Law of Conservation of Energy, this observation allowed us to measure the elastic energy (ϵ) stored in the strand, since $\epsilon = (\frac{1}{2})mv_0^2$, where $v_0 = 13$ μm s^{-1} is the initial velocity, $m = (4/3\pi)\, R_P^3\, \rho$ is the mass, and $\rho = 1.1$ g cm^{-3} is the density of a microsphere. The energy of this strand of length, $L = 9.8$ μm, is calculated to be remarkably small: $\epsilon = 3.2 \times 10^{-25}$ J. The magnitude of the stored energy may provide some indication of underlying mechanical and chemical processes. During plasmolysis, work is done (due to the differential osmotic pressure) to lengthen the strand; however, during deplasmolysis, the strand does not appear to experience osmotic re-compression. It therefore requires more energy to plasmolyze than to deplasmolyze the cell, and, thus, the deplasmolyzed state is energetically more favorable, as expected. This suggests that the small elastic potential energy that we measured in the broken strand serves only to return a given area of the plasmalemma to its original location adjacent to the cell wall.

Assays for Cytoplasm, ER, and F-Actin in Hechtian Strands

We observed $DiOC_6(3)$ fluorescence in some, but not all, Hechtian strands of *G. biloba* and *N. tabacum*, indicating the presence of ER (data not shown). We did not detect fluorescence in strands using either FDA or phalloidin, indicators of cytoplasm and F-actin, respectively (data not shown).

CONCLUSIONS

We observed Hechtian strands in the callus cells of normal and cold-hardened *G. biloba* and *N. tabacum* cells, as well as in leaf epidermal cells of Arabidopsis. They were not observed in the callus cells of either normal or cold-hardened Arabidopsis, and only about half the cells in the other species had resolvable strands that remained intact at least 1 h after plasmolysis. In cold-hardened *G. biloba*, only a quarter of the cells had strands, although the number density was at least twice as large in those cells (compared with normal *G. biloba* or either normal or cold-hardened *N. tabacum*).

Using laser microsurgery, we ablated a small hole within the cell wall of *G. biloba* and *N. tabacum*. Optical tweezers were then used to insert 1.5-μm diameter microspheres coated with Con A into the PVS of the plasmolyzed cells. The microspheres were brought into contact with Hechtian strands, and binding occurred within 20 s. The binding strength increased by 14% after cold-hardening in *N. tabacum* and by 31% after cold-hardening in *G. biloba* (Table I).

By pulling on a bound microsphere and measuring the displacement of the strand from equilibrium, we determined the strand tension (Figs. 4 and 5). A theoretical model was developed to relate the tension to the number density of strands. Comparing the data for *G. biloba* with the model, we concluded that the number density of cold-hardened strands was more likely to decrease with increasing strand length, due to either breaking or merging, than normal strands. While the data for cold-hardened *N. tabacum* also suggested a decreasing number density with strand length, insufficient data were available to make a comparison with normal strands. We propose that strand coalescence provides a mechanism to maintain the integrity of the Hechtian strands during plasmolysis (which may naturally occur when the plant dehydrates). Given the evidence of enhanced combining of neighboring strands and enhanced binding of microspheres to glyco-bearing structures on the strand, we suggest further explorations to determine whether the glyco structures are responsible for the merger.

Surprisingly, we found little difference between the spring constants of *G. biloba* (an ancient gymnosperm that survives winters to -30°C) and *N. tabacum* (an annual non-hardy angiosperm). According to our model, this indicates that the initial number density of strands is roughly the same in both species. Indeed, the measured number densities were nearly identical in normal and hardened *N. tabacum* and normal *G. biloba*; however, the density was approximately 2.3 times higher in cold-hardened *G. biloba*. Due to the large variation in the data, it was not possible to correlate this increased number density with either the strand tension or the spring constant.

We also found that the Hechtian strands break easily under rapid plasmolysis, and concluded that the strands are not effective at conserving the excess plasmalemma. We never observed strands coalescing while the cell was plasmolyzed, only plasmalemma sheets in cold-hardened cells were observed to merge. We also did not observe new strands being formed to replace broken ones. We observed many cells after prolonged plasmolysis (>60 min) that had fewer strands, and sometimes these remaining strands appeared thicker, suggesting that merging occurs (Fig. 6).

The ability to attach microspheres to Hechtian strands adds a new dimension to the study of plant physiology—events can be monitored virtually in situ. Typical microinjection methods would require boring a larger hole to allow a micropipette with a microsphere to enter a cell without having the microsphere scraped off as the micropipette is pushed through the wall. With optical tools, a microsphere can be maneuvered onto a 50-nm-thick Hechtian strand that is barely resolvable with visible optics. Using the microsphere as a physical handle, forces of piconewton magnitudes were measured, allowing us to conclude that there are very specific alterations that occur with cold acclimation in the connections between the plasmalemma and cell wall.

ACKNOWLEDGMENTS

We thank a former graduate student, K. Gahagan, now at Los Alamos National Labs (Los Alamos, NM), for helping to develop the optical system. We also are grateful to D. Walcerz (Applied Sciences Department, York College, York, PA) for the flow chamber; G. Li (Worcester Polytechnic Institute [WPI] Physics Department) for assistance with calibration experiments; A. Walther (WPI Physics Department) for suggestions on microscopy; J. Petruccelli (WPI Math Department) for assistance with the statistical analysis; and K. Wobbe (WPI Chemistry and Biochemistry Department) for donating Arabidopsis seeds and technical suggestions.

Received September 30, 1999; accepted November 15, 1999.

LITERATURE CITED

Akama K, Shiraishi H, Ohta S, Nakamura K, Okada K, Shimura Y (1992) Efficient transformation of *Arabidopsis thaliana*: comparison of the efficiencies with various organs, plant ecotypes, and *Agrobacterium* strains. Plant Cell Rep **12:** 7–11

Alberdi M, Corcuera LJ (1991) Cold acclimation in plants. Phytochemistry **30:** 3177–3184

Ashkin A, Dziedzic JM (1989) Internal cell manipulation using infrared traps. Proc Natl Acad Sci USA **86:** 7914–7918

Ashkin A, Dziedzic JM, Bjorkholm JE, Chu S (1986) Observations of a single-beam gradient force optical trap for dielectric particles. Optics Lett **11:** 288–290

Attree SM, Sheffield E (1985) Plasmolysis of *Pteridium* protoplasts: a study using light and scanning-electron microscopy. Planta **165:** 151–157

Bachewich CL, Heath IB (1997) Differential cytoplasm–plasmalemma–cell wall adhesion patterns and their relationships to hyphal tip growth and organelle motility. Protoplasma **200:** 71–86

Barak LS, Yocum RR, Nothnagel EA, Webb WW (1980) Fluorescence staining of the actin cytoskeleton in living cells with 7-nitrobenz-2-oxa-1,3-diazole-phallacidin. Proc Natl Acad Sci USA **77:** 980–984

Bower FO (1883) On plasmolysis and its bearing upon the relations between cell wall and protoplasm. Q J Microsc Sci **23:** 151–167

Buer CS (1998) Applications of optical manipulation in plant biology. PhD thesis. Worcester Polytechnic Institute, Worcester, MA

Buer CS, Gahagan KT, Swartzlander GA Jr, Weathers PJ (1998) Insertion of microscopic objects through plant cell walls using laser microsurgery techniques. Biotechnol Bioeng **60:** 348–355

Burgess J (1971) Observations on structure and differentiation in plasmodesmata. Protoplasma **73:** 83–95

Canut H, Carrasco A, Galaud J-P, Cassan C, Boussou H, Vita N, Ferrara P, Pont-Lezica R (1998) High affinity RGD-binding sites at the plasma membrane of *Arabidopsis thaliana* links the cell wall. Plant J **16:** 63–71

Carrier D-J, Cosentino G, Neufeld R, Rho D, Weber M, Archambault J (1990) Nutritional and hormonal requirements of *Ginkgo biloba* embryo-derived callus and suspension cell culture. Plant Cell Rep **8:** 635–638

Castonguay Y, Nadeau P, Michaud R (1998) Differential accumulation of oligosaccharides and freezing tolerance of alfalfa. *In* PH Li, THH Chen, eds, Plant Cold Hardiness. Plenum Press, New York, pp 293–299

Chang P-F, Damsz B, Kononowicz AK, Reuveni M, Chen Z, Xu Y, Hedges K, Tseng CC, Singh NK, Narasimhan ML, Hasegawa PM, Bressan RA (1996) Alterations in cell membrane structure and expression of a membrane-associated protein after adaptation to osmotic stress. Physiol Plant **98:** 505–516

De Boer AH, Van Duijn B, Giesberg P, Wegner L, Obermeyer G, Köhler K, Linz KW (1994) Laser microsurgery: a versatile tool in plant (electro) physiology. Protoplasma **178:** 1–10

Drake G, Carr DJ, Anderson WP (1978) Plasmolysis, plasmodesmata, and the electrical coupling of oat coleoptile cells. J Exp Bot **29:** 1205–1214

Felgner H, Frank R, Schliwa M (1996) Flexural rigidity of microtubules measured with the use of optical tweezers. J Cell Sci **109:** 509–516

Gilmore SJ, Hajela RK, Thomashow MF (1988) Cold acclimation in *Arabidopsis thaliana*. Plant Physiol **87:** 745–750

Goldstein IJ, Poretz RD (1986) Isolation, physiochemical characterization, and carbohydrate-binding specificity of lectins. *In* IE Leiner, N Sharon, IJ Goldstein, eds, The Lectins. Academic Press, San Diego, pp 33–67

Goosen-De Roo L (1973) The fine structure of the protoplast in primary tracheary elements of the cucumber after plasmolysis. Acta Bot Neerl **22:** 467–485

Grabski S, Xie XG, Holland JF, Schindler M (1994) Lipids trigger changes in the elasticity of the cytoskeleton in plant cells: a cell optical displacement assay for live cell measurements. J Cell Biol **126:** 713–726

Gunning BES, Steer MW (1996) Plant Cell Biology, Structure and Function, plate 16. Jones and Bartlett, Sudbury, MA

Guy CL (1990) Cold acclimation and freezing tolerance: role of protein metabolism. Annu Rev Plant Physiol Plant Mol Biol **41:** 187–223

Heath IB (1987) Preservation of a labile cortical array of actin filaments in growing hyphal tips of the fungus *Saprolegnia ferax*. Eur J Cell Biol **44:** 10–16

Hecht K (1912) Studien über den Vorgang der Plasmolyse. Beitr Biol Pflanz **11:** 137–191

Henry CA, Jordan JR, Kropf DL (1996) Localized membrane-wall adhesions in *Pelvetia* zygotes. Protoplasma **190:** 39–52

Hepler PK, Palevitz BA, Lancelle SA, McCauley MM, Lichtscheidl I (1990) Cortical endoplasmic reticulum in plants. J Cell Sci **96:** 355–373

Hoffmann F (1996) Laser microbeams for the manipulation of plant cells and subcellular structures. Plant Sci **113:** 1–11

Hughes MA, Dunn MA (1996) The molecular biology of plant acclimation to low temperature. J Exp Bot **47:** 291–305

Johnson SL (1994) Tissue culture of *Ginkgo biloba*. Bios **65:** 193–200

Johnson-Flanagan AM, Singh J (1986) Membrane deletion during plasmolysis in hardened and non-hardened plants. Plant Cell Environ **9:** 299–305

Kell A, Glaser RW (1993) On the mechanical and dynamic properties of plant cell membranes: their role in growth, direct gene transfer, and protoplast fusion. J Theor Biol **160:** 41–62

Kelly SG (1993) Fundamentals of Mechanical Vibrations. McGraw-Hill, New York, p 45

Knebel W, Quader H, Schnepf E (1990) Mobile and immobile endoplasmic reticulum in onion bulb epidermis cells: short- and long-term observations with a confocal laser scanning microscope. Eur J Cell Biol **52:** 328–340

Kucik DF, Kuo SC, Elson EL, Sheetz MP (1991) Preferential attachment of membrane glycoproteins to the cytoskeleton at the leading edge of lamella. J Cell Biol **114:** 1029–1036

Kuroda K (1990) Cytoplasmic streaming in plants. Int Rev Cytol **121:** 267–307

Landau LD, Lifshitz EM (1959) Theory of Elasticity. Addison-Wesley, Reading, MA, p 91

Lee-Stadelmann OY, Stadelmann EJ (1989) Plasmolysis and deplasmolysis. Methods Enzymol **174:** 225–246

Li PH, Chen TH, eds (1998) Plant Cold Hardiness. Molecular Biology, Biochemistry, and Physiology. Plenum Press, New York

Lichtscheidl IK, Lancelle SA, Hepler PK (1990) Actin-endoplasmic reticulum complexes in *Drosera*. Their structural relationship with the plasmalemma, nucleus, and organelles in cells prepared by high pressure freezing. Protoplasma **155:** 116–126

Liebe S, Quader H (1994) Myosin in onion (*Allium cepa*) bulb scale epidermal cells: involvement in dynamics of organelles and endoplasmic reticulum. Physiol Plant **90:** 114–124

Linsmaier EM, Skoog F (1965) Organic growth factor requirements of tobacco tissue cultures. Physiol Plant **18:** 100–128

Mehta AD, Finer JT, Spudich JA (1998) Reflections of a lucid dreamer: optical trap design considerations. *In* MP Sheetz, ed,

Laser Tweezers in Cell Biology. Academic Press, San Diego, pp 47–69

Munson BR, Young DF, Okiishi TH (1994) Fundamentals of Fluid Mechanics, Ed 2. John Wiley & Sons, New York, p 14

Murashige T, Skoog F (1962) A revised medium for rapid growth and bioassays with tobacco tissue cultures. Physiol Plant **15:** 473–479

Nägeli C (1855) Pflanzenphysiologische Untersuchungen. Heft 1, Schulthess, Zürich, pp 1–35 (Quoted in Bower, 1883)

Niu X, Damsz B, Kononowicz AK, Ressan RA, Hasegawa PM (1996) NaCl-induced alterations in both cell structure and tissue-specific plasma membrane H^+-ATPase gene expression. Plant Physiol **111:** 679–686

Oparka KJ (1994) Tansley Review no. 67: Plasmolysis: new insights into an old process. New Phytol **126:** 571–591

Oparka KJ, Prior DAM, Crawford JW (1994) Behaviour of plasma membrane, cortical ER, and plasmodesmata during plasmolysis of onion epidermal cells. Plant Cell Environ **17:** 163–171

Oparka KJ, Roberts AG, Roberts IM, Prior DAM, Cruz SS (1996) Viral coat protein is targeted to, but does not gate, plasmodesmata during cell-to-cell movement of potato virus X. Plant J **10:** 805–813

Pont-Lezica RF, McNally JG, Pickard BG (1993) Wall-to-membrane linkers in onion epidermis: some hypotheses. Plant Cell Environ **16:** 111–123

Plowe JQ (1931) Membranes in the plant cell. I. Morphological membranes at protoplasmic surfaces. Protoplasma **12:** 196–220

Pringsheim N (1854) Untersuchungen über den Bau und Bildung der Pflanzenzelle. Abt 1: Grundleinen einer Theorie der Pflanzanzelle, Hershwald, Berlin, pp 12–13 (Quoted in Bower, 1883)

Quader H, Schnepf E (1986) Endoplasmic reticulum and cytoplasmic streaming: fluorescence microscopical observations in adaxial epidermis cells of onion bulb scales. Protoplasma **131:** 250–252

Scarth GW (1941) Dehydration injury and resistance. Plant Physiol **16:** 171–179

Schindler M (1995) Cell optical displacement assay (CODA): measurements of cytoskeletal tension in living plant cells with a laser optical trap. Methods Cell Biol **49:** 71–84

Schindler M, Meiners S, Cheresh DA (1989) RGD-dependent linkage between plant cell wall and plasma membrane: consequences for growth. J Cell Biol **108:** 1955–1965

Sheetz MP, ed (1998) Laser tweezers in cell biology. Methods Cell Biol **55**

Singer S, Nicolson G (1972) The fluid mosaic model of the structure of cell membranes. Science **175:** 720–731

Sitte P (1963) Zellfeinbau bei Plasmolyse. II. Der Feinbau der Elodea-Blattzellen bei Zucker- und Ionenplasmolyse. Protoplasma **57:** 304–333

Staehelin LA (1997) The plant ER: a dynamic organelle composed of a large number of discrete functional domains. Plant J **11:** 1151–1165

Svoboda K, Block SM (1994) Biological applications of optical forces. Annu Rev Biophys Biomol Struct **23:** 247–285

Terasaki M, Reese TS (1992) Characterization of endoplasmic reticulum by co-localization of BiP and dicarbocyanine dyes. J Cell Sci **101:** 315–322

Thomashow MF (1998) Role of cold-responsive genes in plant freezing tolerance. Plant Physiol **118:** 1–17

Tokuhisa J, Wu J, Miquel M, Xin Z, Browse J (1998) Investigating the role of lipid metabolism in chilling and freezing tolerance. *In* PH Li, THH Chen, eds, Plant Cold Hardiness. Plenum Press, New York, pp 153–169

Uemura M, Steponkus PL (1998) Effect of cold acclimation on membrane lipid composition and freeze-induced membrane destabilization. *In* PH Li, THH Chen, eds, Plant Cold Hardiness. Plenum Press, New York, pp 171–179

Walcerz DB, Diller KR (1991) Quantitative light microscopy of combined perfusion and freezing processes. J Microsc **161:** 297–311

Widholm JM (1972) The use of fluorescein diacetate and phenosafranine for determining viability of cultured plant cells. Stain Technol **47:** 189–194

Wright WH, Sonek GJ, Berns MW (1994) Parametric study of the forces on microspheres held by optical tweezers. Appl Optics **33:** 1735–1748

Zabotin AI, Barisheva TS, Zabotina OA, Larskaya IA, Lozovaya VV, Beldman G, Voragen AGJ (1998) Alterations in cell walls of winter wheat roots during low temperature acclimation. J Plant Physiol **152:** 473–479